

Structural Changes along and above the Yrast Line of ^{154}Dy

W. C. Ma,⁽¹⁾ M. A. Quader,⁽²⁾ H. Emling,^{(1),(a)} T. L. Khoo,⁽¹⁾ I. Ahmad,⁽¹⁾ P. J. Daly,⁽²⁾ B. K. Dichter,^{(1),(b)} M. Drigert,^{(3),(c)} U. Garg,⁽³⁾ Z. W. Grabowski,⁽²⁾ R. Holzmann,^{(1),(a)} R. V. F. Janssens,⁽¹⁾ M. Piiparinen,^{(2),(d)} W. H. Trzaska,⁽²⁾ and T.-F. Wang⁽¹⁾

⁽¹⁾Argonne National Laboratory, Argonne, Illinois 60439

⁽²⁾Purdue University, West Lafayette, Indiana 47907

⁽³⁾University of Notre Dame, Notre Dame, Indiana 46556

(Received 29 December 1987)

States in ^{154}Dy have been located up to $I^\pi=48^+$ and their lifetimes measured. Marked structural changes occur along the yrast line with a transition from prolate to oblate shape, followed by an unexpected return to moderate collectivity at the highest spins. Structural changes with increasing energy above the yrast line are also observed.

PACS numbers: 21.10.Pc, 21.10.Re, 23.20.Ck, 27.70.+q

Rapid rotation may induce dramatic structural changes in some nuclei. The transitional nuclei, which lie in the regions between spherical and deformed nuclei, should be particularly susceptible to stresses arising from rapid rotation. Thus, properties of such nuclei provide a stringent test of nuclear models. The $N=88$ isotones, which bridge the sudden change from oblate shapes for $N \leq 86$ to prolate shapes for $N \geq 90$, have been a fertile testing ground. They generally have slightly prolate shapes at low spins, but switch to oblate shapes at higher spins.¹⁻³ Theory² accounts for this switch in terms of band termination, a process where the shape associated with a given configuration having initial prolate deformation changes until it reaches the oblate limit. This band-termination picture has so far been checked mainly by comparisons with the energy levels of yrast states of nuclei in the transitional region. For a more rigorous test of theoretical models it is important to measure both yrast and nonyrast levels and, particularly, to determine lifetimes, which provide a direct measure of collectivity. It is also of considerable interest for our understanding of nuclear structure to measure the properties of states at higher spin to ascertain if the oblate coupling scheme persists beyond the maximum spin which can be generated by the valence nucleons.

With these motivations, we have identified levels in $^{154}\text{Dy}_{88}$ to very high spin ($I^\pi=48^+$) and have also measured the state and feeding lifetimes. The level scheme and $B(E2)$ values confirm the previously observed prolate-to-oblate transition.^{1,2} However, at the highest spins a feature not predicted by theory is observed: There is a return to collective behavior at $I=40$.

High-spin states of ^{154}Dy were populated via the reaction $^{122}\text{Sn}(^{36}\text{S},4n)$ with a 165-MeV beam from ATLAS (Argonne Tandem Linac Accelerator System). Two types of targets (^{122}Sn enrichment $> 92\%$) were used: a stack of four self-supporting foils which allowed the residues to recoil into vacuum, and a target evaporated on a Pb backing, in which the residues stopped in ≈ 2 ps. In each case, the total Sn thickness was ≈ 1 mg cm^{-2} . The

decay γ 's were detected with use of the Argonne-Notre Dame γ -ray facility consisting of eight bismuth germanate Compton-suppressed Ge spectrometers, of which three were positioned at 34° , two at 90° , and three at 146° with respect to the beam direction. A central array of fourteen bismuth germanate hexagons, with a detection efficiency of 38% for 662-keV γ rays, acted as a multiplicity filter. A total of 135×10^6 true prompt-coincidence events were obtained for the stacked target and 55×10^6 for the backed target. The very clean spectra from the Compton-suppressed Ge spectrometers allowed observation of detailed line shapes for the γ rays from the backed-target data. Hence lifetime analysis for the fast transitions (from states with $I^\pi=38^+-44^+$) was possible. The stacked-target data are necessary mainly for the fast γ rays, as some of the lines were significantly smeared from Doppler broadening in the backed-target spectra. Finally, lifetimes of longer-lived states (with $I^\pi=34^+-38^+$) were measured with the recoil distance method with use of the plunger described by Azgüi.⁴ Details of the experiments will be described in a forthcoming paper.

The level scheme for ^{154}Dy deduced from the present experiment is shown in Fig. 1. The ordering of the transitions is based on coincidence relationships, cascade-crossover connections, intensity arguments and, for the highest positive-parity levels, decay-time considerations. Relative γ -ray intensities were extracted from the coincidence spectra obtained with the stacked target. Spin and parity assignments are based on directional correlation ratios.⁵ All the transitions reported in Ref. 2 are observed, although some of them are now placed differently in the level scheme. The positive-parity sequence has been extended to spin 48, and the negative-parity sequence to spin 42 (or 43). More than fifty new lines have been assigned, so that many new nonyrast states are located.

The γ -ray intensity drops quickly at the highest spins of the positive-parity sequence. Although the intensity of the transition depopulating the 44^+ state is still quite

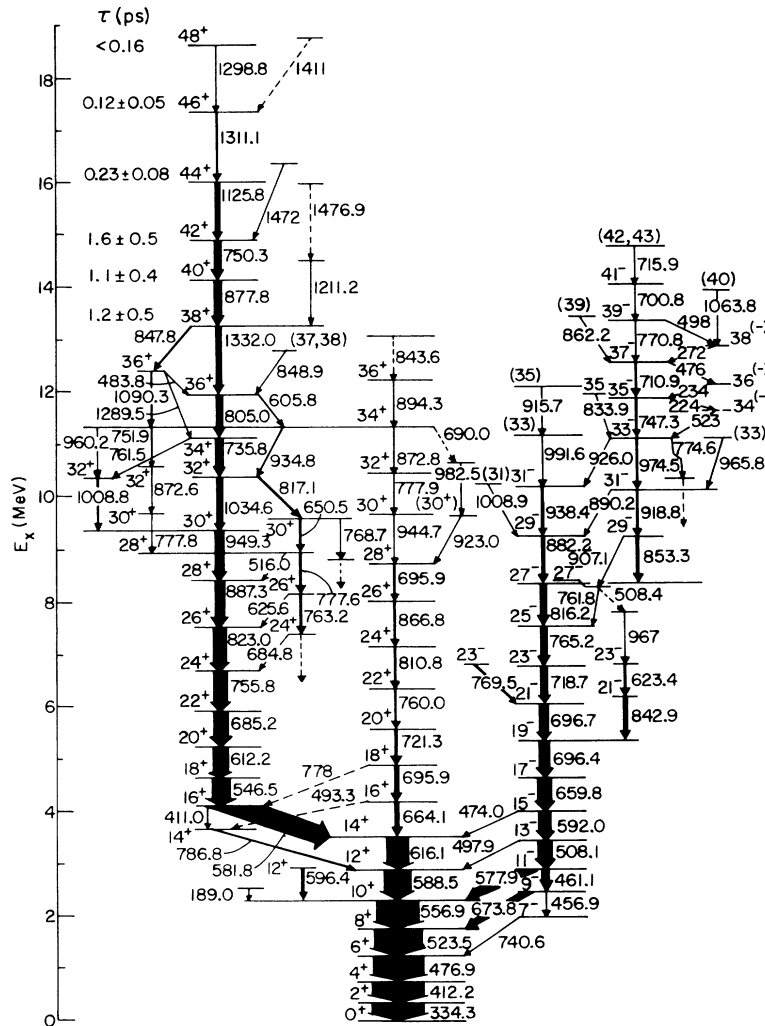


FIG. 1. ^{154}Dy level scheme. Lifetimes for the higher-spin positive-parity levels are also given.

high (9%), for $I^\pi > 44^+$ the decay pathway fragments. Thus the 1311- and 1299-keV transitions at higher spin have intensities of only 4% and $< 2\%$, respectively.

In the negative-parity sequence, the placement of the 853-keV ($29^- \rightarrow 27^-$) transition is confirmed by all coincidence considerations while it was not included in the main decay cascade by previous works.^{1,2} In addition to the two parallel γ -ray sequences populating the 19^- and 27^- states in the main cascade, an interesting feature is the presence of a series of dipole transitions between spin 33^- and 39^- .

By comparing the backed-target data obtained from the forward, backward, and 90° detectors, Doppler-shifted line shapes can be seen clearly for the strong transitions above spin 36^+ in the positive-parity cascade. Figure 2 shows an example from the $44^+ \rightarrow 42^+$ transition. The line shapes allow for the extraction of state and feeding lifetimes by the Doppler-shift attenuation method. The slowing-down process of recoils in the

target and backing material was calculated with the Northcliffe-Schilling⁶ stopping powers after normalization to the α stopping powers of Ziegler and Chu.⁷ The nuclear stopping was also included following Lindhard *et al.*⁸ with low-energy ion scattering corrections from Blaugrund.⁹ A computer code was written to fit the measured Doppler-broadened line shapes. The measured lifetimes are indicated in Fig. 1 and also in Fig. 3. (A more sophisticated Monte Carlo treatment¹⁰ of the slowing-down process yields the same results within errors.) For the weak 1299-keV transition, only an upper limit on its deexciting lifetime was obtained, which, however, clearly shows that it is fast. The lifetimes of the $I^\pi = 38^+$ state obtained from the Doppler-shift attenuation and recoil distance methods were in excellent agreement.

In the γ -ray intensities extracted from the backed and stacked targets clear differences were found not only for the fast γ rays above $I^\pi = 36^+$, but also for the transi-

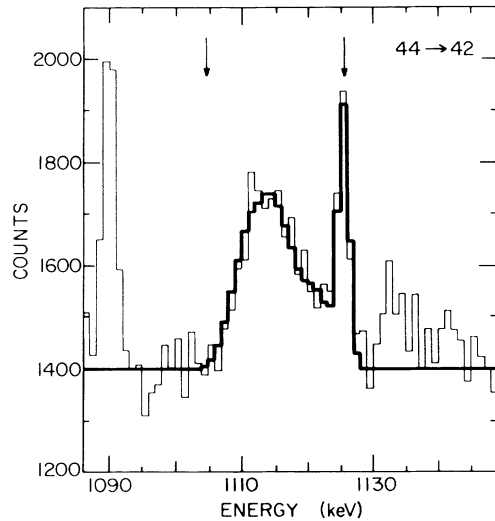


FIG. 2. Line shape of 1125-keV transition observed at 146° . Experiment, thin line; calculation, thick line. Arrows indicate energies corresponding to full and zero Doppler shift.

tions between spin 22^+ and 32^+ in the positive-parity sequence. (For the backed target only the intensity of the stopped component was used, so that if a γ ray contains a fast Doppler-broadened component its intensity should be smaller than that from the stacked target.) As the effective lifetimes of the lower-spin states are very long (> 10 ps), the fast components in their deexciting γ rays must come from fast "side feeding" (i.e., feeding into the state under consideration from all other unobserved levels) ($\tau_{\text{feed}} < 1$ ps), in agreement with the results of Azgui *et al.*⁴

The observation of both yrast and several nonyrast states makes a stringent comparison with theory² possible. Figure 3 is a plot of energies versus spin for the positive-parity levels; transitions connecting the levels are also indicated. The ground-state band (GSB) is seen to be crossed at $I^\pi = 16^+$ by an aligned $\nu i_{13/2}$ S band, which then continues as the yrast structure to $I^\pi = 32^+$, while the GSB continues as an excited band to $I^\pi = 26^+$. Both bands are crossed at these spins by structures whose irregular energies and lifetimes (where measured) suggest the approach toward aligned-particle configurations. For $I^\pi = 38^+ - 48^+$, yet another structure becomes yrast, with a preferential reduced- $E2$ decay to the 36_3^+ level. The transitions of this last structure, shown as medium arrows in Fig. 3, exhibit moderate collectivity [$Q_t = 198 - 243 e \text{ fm}^2$, 29-43 Weisskopf units (W.u.)]. A comparison of the results shown in Fig. 3 with a similar plot for the calculated levels—see Fig. 7 in Ref. 2—shows good agreement in the overall features up to $I^\pi = 36^+$, the maximum valence spin. By locating the nonyrast levels we have thus been able to demonstrate the predicted descent of the oblate aligned-particle configurations towards the yrast line and the consequent

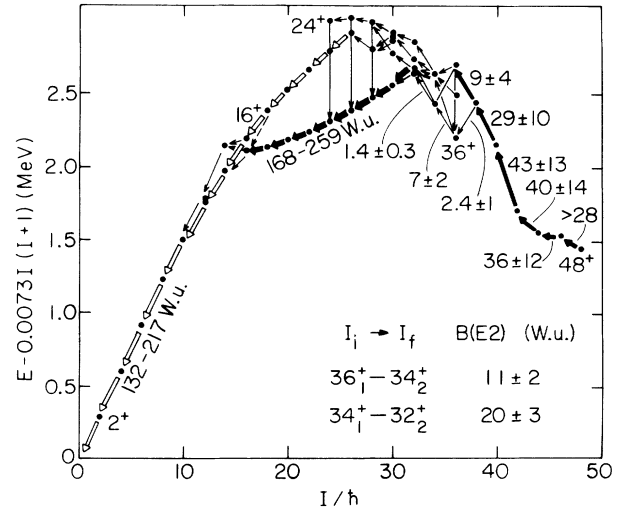


FIG. 3. Level energy (after subtraction of a rotational term) vs spin for positive-parity levels; connecting transitions are shown, thereby exhibiting the structural connections of states. Transitions within the ground band, the S band, and the moderately collective band at the highest spins are shown as open, heavy, and medium arrows, respectively; demonstrated or probable single-particle transitions are shown as thin lines. The numbers by the highest-spin transitions are $B(E2)$ values in Weisskopf units (W.u.); $B(E2)$ values for the ground and S bands are from Refs. 1 and 4.

crossing of the GSB and S band. In the theory a terminating-band picture is predicted at the higher spins, where along a band with given configuration the shape changes from prolate ($\gamma = 0^\circ$) to oblate ($\gamma = 60^\circ$) through a triaxial excursion (with intermediate values of γ). The three consecutive yrast transitions, $34_1^+ \rightarrow 32_1^+$, $36_1^+ \rightarrow 34_1^+$, and $38_1^+ \rightarrow 36_1^+$ ($E_\gamma = 761, 805,$ and 1332 keV) are of single-particle type (1.4, 7, and 2.4 W.u., respectively). The negative-parity level energies (not displayed in Fig. 3) show similarly good agreement with theory; in particular, the unusual series of dipole transitions between $I^\pi = 33^-$ and 39^- is in excellent accord with the theoretical predictions² of signature degenerate bands.

However, above spin 38 the agreement with theory appears to break down for the positive-parity states: The moderately collective structures observed are quite different from the predominantly oblate single-particle yrast states predicted.² There is a possibility that the single-particle states mix with higher-lying collective bands to give rise to the observed structures. However, the extended sequence of five collective transitions would be difficult to explain in this manner since the collective states are calculated² to lie 0.8-2.7 MeV higher.

While collective components have been observed in the unresolved γ spectra of transitional nuclei at high spin, this is the first time that a change from single-particle to

collective behavior has been observed along the yrast line in the discrete-line spectrum. The unexpected return to collectivity at the highest spin stands out as a general challenge for theory to explain. The moderate collectivity may suggest a triaxial shape. The favoring of the collective structure rather than the expected oblate aligned-particle configurations may suggest that the cost of the promotion of particles into higher-lying orbitals (possibly from the next major shell¹¹) is compensated by deformation. This structure may represent the initial stage in the excursion towards the larger deformation present in the quasicontinuum states in ¹⁵⁴Dy (Holzmann *et al.*¹²) or those prevalent in the heavier prolate Dy isotopes. An alternative explanation is that the configurations of this structure do, in fact, correspond to the calculated oblate aligned-particle states with energy minima at $\gamma=60^\circ$. If this is the case, the moderate collectivity may be due to very flat potential-energy surfaces extending into the triaxial plane.

In summary, an impressive series of nuclear-structure changes along the yrast line have been observed in ¹⁵⁴Dy: from the GSB to an aligned $\nu i_{13/2}$ band, to oblate aligned-particle configurations, and finally an unexpected return to moderately collective states. The observation of several nonyrast levels has also made it possible to see (Fig. 3) a change of structure with an increase in excitation energy above the yrast line, and to follow the descent of oblate aligned-particle configurations towards the yrast line with increasing spin until they cross both the GSB and $\nu i_{13/2}$ band. The theoretical predictions in the band-terminating picture² impressively account for the observed features for $I \leq 36$. However, the return of collectivity at higher spins was not predicted, thereby

raising challenging questions about the nature of collectivity at the highest spins.

We acknowledge helpful conversations with T. Bengtsson, I. Ragnarsson, and M. Riley. This work was supported by the U. S. Department of Energy, Nuclear Physics Division, under Contracts No. W-31-109-Eng-38 and No. DE AC02-76ER01672, and the National Science Foundation under Grant No. PHY84-16025.

^(a)Present address: GSI, Darmstadt, West Germany.

^(b)Present address: Panametrics, Inc., Waltham, MA 02254.

^(c)Present address: Idaho National Engineering Laboratory, Idaho Falls, ID 83415.

^(d)Permanent address: University of Jyväskylä, Jyväskylä, Finland.

¹A. Pakkanen *et al.*, Phys. Rev. Lett. **48**, 1530 (1982).

²H. W. Cranmer-Gordon *et al.*, Nucl. Phys. **A465**, 506 (1987).

³F. S. Stephens *et al.*, Phys. Rev. Lett. **54**, 2584 (1985); C. Baktash, Phys. Rev. Lett. **54**, 978 (1985); S. Patel, Phys. Rev. Lett. **57**, 62 (1986).

⁴F. Azgui *et al.*, Nucl. Phys. **A439**, 573 (1985).

⁵K. S. Krane *et al.*, Nucl. Data Tables **11**, 351 (1973).

⁶L. C. Northcliffe and R. F. Schilling, Nucl. Data Tables A **7**, 233 (1970).

⁷J. F. Ziegler and W. K. Chu, At. Data Nucl. Data Tables **13**, 463 (1974).

⁸J. Lindhard *et al.*, Mat. Fys. Medd. K. Dan. Vidensk. Selsk. **33**, No. 14 (1963).

⁹A. E. Blaugrund, Nucl. Phys. **88**, 501 (1966).

¹⁰H. Emling *et al.*, to be published.

¹¹M. A. Deleplanque, Nucl. Phys. **A448**, 495 (1986).

¹²R. Holzmann *et al.*, to be published.